

New insights into an Old Molecule: Interaction Energies of Theophylline

Crystal Forms

Katharina Fücke^a, Garry J. McIntyre^{a,b}, Clive Wilkinson^{a,c}, Marc Henry^d, Judith A.K. Howard^a, Jonathan

W. Steed^{*a}

^a Department of Chemistry, Durham University, Science Site, South Road, Durham DH1 3LE, United Kingdom. Email: Jon.Steed@durham.ac.uk

^b The Bragg Institute, Australian Nuclear Science and Technology Organisation, Locked Bag 2001, Kirrawee DC NSW 2234, Australia

^c Institut Laue-Langevin, 6 rue Jules Horowitz, BP 156, 38042 Grenoble Cedex 9, France

^d Institut Le Bel, Université Louis Pasteur, 4 Rue Blaise Pascal, 67070 Strasbourg Cedex, France

Abstract

The asthma therapeutic theophylline exists in at least three anhydrous polymorphs and a monohydrate. The single-crystal X-ray structure of the high-temperature polymorph form I is presented for the first time and the energetic relationship between forms I and II is investigated using the partial charges and chemical hardness analysis (PACHA) algorithm. It is shown that the interactions in the form I crystal network are stronger, especially the hydrogen bond. The single-crystal neutron structure of the monohydrate demonstrates static disorder of the water molecule as well as dynamic disorder of the methyl groups. PACHA investigations based on the neutron coordinates reveal that the homomeric interactions in this form are stronger than the interaction of the water with the host molecules. The dehydration of the hydrate should thus leave the theophylline network intact, explaining the isomorphous powder X-ray diffractograms of the monohydrate and its dehydrated form III.

Keywords: Hydrate, neutron diffraction, polymorphism, lattice-energy calculation, Laue diffraction

Introduction

Polymorphism, the phenomenon of different crystal forms occurring for a specific molecule, has been known for nearly 200 years.¹ Different crystal forms can vary widely in their physico-chemical characteristics, such as melting point, solubility, chemical and physical stability. This variation can prove problematic especially in pharmaceutical compounds, because it can cause processing problems, instability in the final formulation or influence the drug's bioavailability because of the differing solubility of different polymorphic forms.²⁻⁵ The choice of the wrong crystal form thus causes severe problems and can cost the pharmaceutical company large amounts of money in 'damage limitation'.^{6,7}

In addition to 'pure' polymorphs, crystals may contain solvent of crystallisation resulting in various solvate forms, or hydrates in the special case of the inclusion of water.⁸ The incorporated solvent can vary in its interaction with the host molecules in the crystal and exhibit varying stability towards desolvation. Moreover, solvates show the lowest solubility in the solvent they incorporate.⁹ In the case of hydrate formation of drugs this can have considerable effects on the bioavailability of the compound, as all medicines need to ultimately dissolve in aqueous human or animal body fluids. There is considerable current interest in the study of water clusters in crystalline hydrates in order to understand the homomeric and heteromeric interactions of the water and the host molecules.^{8,10-14}

It is increasingly apparent that many compounds can exist in more than one crystal form and identification and analysis of every form (particularly the thermodynamically stable form under a given set of conditions)¹⁵ is essential for manufacturing, storage and intellectual property considerations.^{3,16} Discovery of the full range of crystal forms of any given compound is usually time-consuming and expensive, and even after extensive screening it is difficult to be certain that the process is complete and every possible form has been identified. In this regard, computational

crystal-structure prediction is a useful and fast-growing field,¹⁷ and has developed from small rigid compounds to more complex multi-component systems like hydrates.^{18,19} Moreover novel approaches such as supramolecular gel crystallization can increase the chance of discovering the difficult-to-nucleate solid forms.²⁰ However, without experimentally obtained crystal structures, computational *ab initio* prediction cannot be validated and the factors governing the stability of a particular solid form cannot be understood. In this study we report the structure of the elusive high-temperature form I of the well-known drug theophylline and probe its relationship with the room temperature form II by *ab initio* lattice energy calculations based on the crystallographic coordinates obtained by X-ray and neutron crystallography.

Theophylline (THEO, Figure 1) has been known since 1888,²¹ when it was first extracted from tea leaves, and it has been in pharmaceutical use since 1902. THEO is a strong bronchospasmolyticum and bronchodilatator, and is mainly used as a treatment of bronchial asthma. The compound is listed in both the European²² and the United States Pharmacopoeia,²³ and the drug and its solid-state properties are still very much in the focus of pharmaceutical research. In crystal-engineering studies THEO is a popular model compound used to explore polymorphism and especially hydrate formation.²⁴⁻²⁷

THEO is reported to crystallise in four different crystal forms. The anhydrous form I is the high-temperature polymorph which is thermodynamically the most stable form above 232 °C.²⁸ Form II is enantiotropically related to form I and is the stable polymorph at room temperature.^{29,30} The crystal structure of this latter form has been solved in the orthorhombic space group $Pna2_1$.^{31,32} The crystal structure of the monohydrate has also been determined and found to be monoclinic, although two space groups ($P2_1$ and $P2_1/n$) have been reported.^{33,34} Upon dehydration under reduced pressure, the monohydrate converts to a third anhydrous crystal form variously named either form I* or form III.^{35,36} The powder X-ray diffractogram of this third form is closely related to the XRPD pattern of the monohydrate. In addition to these crystal forms, THEO readily forms a range of other co-crystals and

is commonly studied as a co-crystal former.³⁷⁻⁴² Recently, a new anhydrous form IV has been reported.^{43,44} However, reproduction of this form following the published procedure of slurry conversion in methanol failed in our hands. Another crystal form has been reported to be obtained by antisolvent precipitation using supercritical CO₂ and CHF₃ as antisolvent.⁴⁵ The authors suggest the new form to be related to the room temperature polymorph form II but distorted and crystallising in a monoclinic rather than orthorhombic symmetry.⁴⁶ This new crystal phase has also been found in theophylline crystallised from methanol or nitromethane, which is pure form II when investigated by powder X-ray diffraction. However, electron microscopy and electron diffraction reveals the existence of the new polymorph as micro-impurity.⁴⁷

In the present work we report the single-crystal neutron structure of theophylline monohydrate and lattice-energy calculations of the hydrate as well as the anhydrous forms I and II using the PACHA algorithm.⁴⁸ The aim is to rationalise the thermodynamic stability and mutual interconversion of the THEO crystal forms using non-empirical energy calculations based on the experimental crystal-structure coordinates.

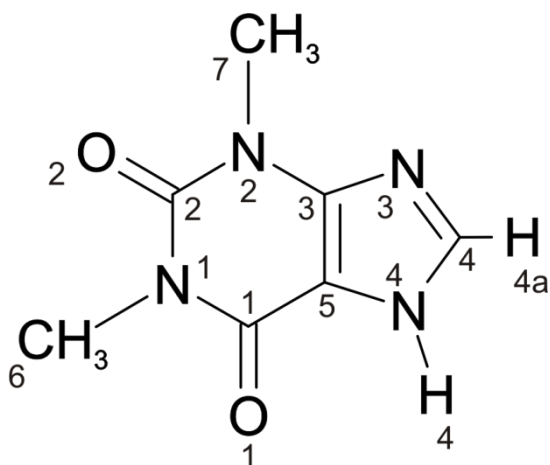


Figure 1 Theophylline molecular structure and numbering scheme used in the crystal structure.

Results and Discussion

Crystal structure analysis of the polymorphic forms I and II

The high-temperature polymorph form I of theophylline was described by Burger and Ramberger in 1979²⁹ but structural data have never been published.⁴⁹ We have succeeded in crystallising single-crystals of sufficient size for X-ray structural analysis from the melt at temperatures above 270 °C, where form I grows slowly as large prismatic crystals. These undergo considerable cracking upon cooling but a sufficiently large intact part of the melt film could be extracted for structure analysis. The crystallographic data are listed in Table 1.

Table 1 Crystallographic data for the three crystal forms of theophylline studied.

Form	I	II	monohydrate	
	X-ray	X-ray	Neutron Laue diffraction	
Formula	C ₇ H ₈ N ₄ O ₂	C ₇ H ₈ N ₄ O ₂	C ₇ H ₈ N ₄ O ₂ · H ₂ O	C ₇ H ₈ N ₄ O ₂ · H ₂ O
<i>M_r</i>	180.17	180.17	198.19	198.19
Crystal system	orthorhombic	orthorhombic	monoclinic	monoclinic
Space group	<i>Pna2</i> ₁	<i>Pna2</i> ₁	<i>P2</i> ₁ / <i>n</i>	<i>P2</i> ₁ / <i>n</i>
<i>T</i> (K)	120(2)	120(2)	120(2)	20(2)
<i>a</i> (Å)	13.087(2)	24.330(1)	4.4605(3)	4.4159(3) ^a
<i>b</i> (Å)	15.579(3)	3.7707(2)	15.3207(9)	15.1675(9) ^a
<i>c</i> (Å)	3.8629(6)	8.4850(5)	13.0529 (7)	12.9224(7) ^a
α (°)	90	90	90	90
β (°)	90	90	97.511(2)	97.511(2)
γ (°)	90	90	90	90
<i>V</i> (Å ³)	787.6(2)	778.43(8)	884.36(9)	858.09(9)
<i>Z</i>	4	4	4	4

density (calc, g/cm ⁻³)	1.520	1.537	1.488	1.534
wavelength (Å)	0.71073	0.71073	0.8 – 5.2	0.8 – 5.2
abs. coef (mm ⁻¹)	0.116	0.118		
F(000)	376	376	256	256
crystal size (mm ⁻³)	0.32 x 0.18 x 0.09	0.98 x 0.14 x 0.08	2.0 x 0.5 x 0.4	2.0 x 0.5 x 0.4
θ range for				
data collection	2.03 – 29.34	1.67 – 30.03		
index ranges	-18 < h < 18	-34 < h < 34	-5 < h < 7	-6 < h < 7
	-21 < k < 14	-5 < k < 5	-23 < k < 24	-23 < k < 24
	-5 < l < 5	-11 < l < 11	-21 < l < 20	-20 < l < 20
reflections collected	6379	9220	5267	4390
independent				
reflections	2139	2267	1549	1519
refinement method		full-matrix least-squares on F^2		
data/restraints/				
parameters	2139/1/124	2267/1/124	1549/0/231	1519/0/205
goodness of fit				
on F^2	0.972	0.955	1.155	2.065
final R indices	R1 = 0.0786	R1 = 0.0416	R1 = 0.0836	R1 = 0.1620
[$I > 2\sigma(I)$]	wR2 = 0.1934	wR2 = 0.0976	wR2 = 0.1731	wR2 = 0.4491
R indices (all data)	R1 = 0.1130	R1 = 0.0569	R1 = 0.0967	R1 = 0.1659
	wR2 = 0.2118	wR2 = 0.1035	wR2 = 0.1741	wR2 = 0.4494
largest diff peak				
and hole [eÅ ⁻¹ /fmÅ ⁻³]	0.311 and -0.317	0.228 and -0.251	1.305 and -1.238	3.038 and -3.114

^a Cell dimensions of the monohydrate structure at 20K are calculated from the cell at 120K with an isotropic shrinking of 1%.

Form I crystallises in the orthorhombic space group $Pna2_1$ with one molecule in the asymmetric unit ($Z' = 1$). The THEO molecule itself is planar, with the methyl substituents in plane with the purine ring. One short hydrogen bond can be detected involving the NH group of the five-membered ring of

one molecule (N4-H4) as donor and a carbonyl group of the six-membered ring of the next molecule as acceptor (C2=O2). Due to this interaction, which connects functional groups on opposite ends of the molecule, the resulting hydrogen-bonded chains connect the THEO molecules like a chain of beads on a string in the (2 0 1) and the (-2 0 1) planes. The hydrogen-bonded chains $\pi\cdots\pi$ -stack on top of each other with a distance of 3.37 Å (a typical distance for this type of compound)⁵⁰ resulting in layers within the structure having the same orientation, with successive layers related through the 2_1 screw axis (Figure 2).

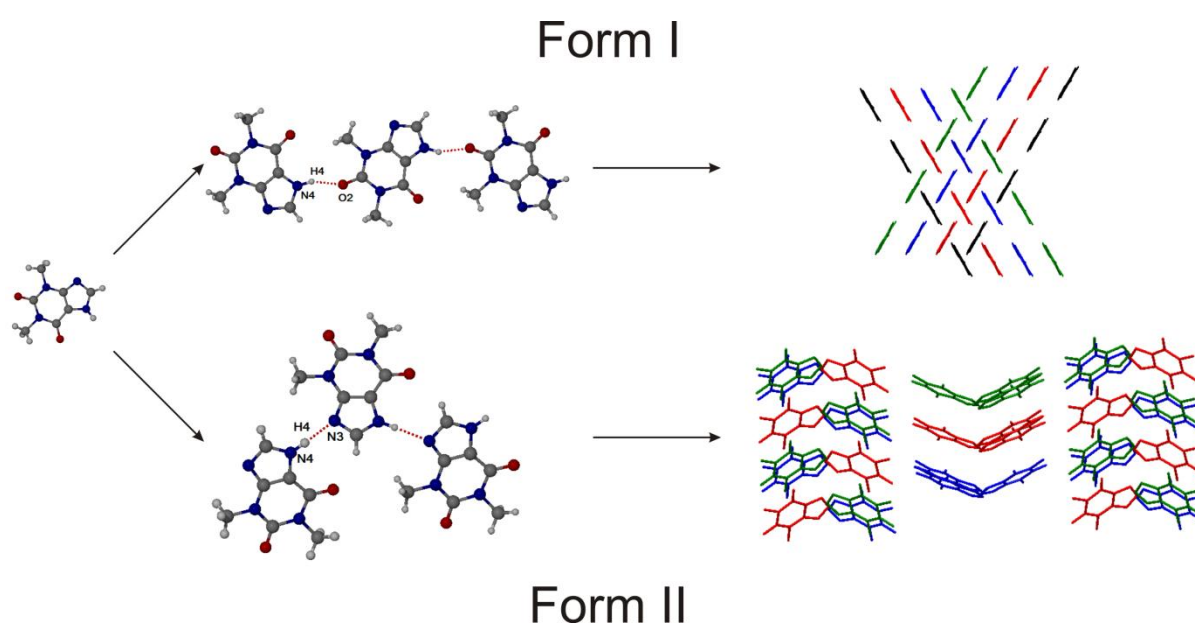


Figure 2 Packing of THEO forms I and II. Each hydrogen bonded chain has its individual colour, hydrogen atoms have been omitted for clarity.

To facilitate comparison, the previously reported crystal structure of form II^{31,32} was redetermined at 120 K from crystals grown by sublimation at 458 K. Form II also crystallises in the orthorhombic spacegroup $Pna2_1$ and has the planar THEO molecule in the same conformation as form I so that these two polymorphs are an example of packing polymorphism, as opposed to conformational polymorphism.⁵¹ Form II like form I shows only one significant hydrogen bond, which in this crystal

form connects from the same donor (N4-H4) to the second nitrogen atom of the five-membered ring of the purine (N3). This different hydrogen bond causes the hydrogen-bonded chains to adopt a zigzag shape (Figure 2). Enclosing the *b*-glide plane, the chains themselves are not planar in contrast to those found in form I and subtend an angle of 134.5° between directly connected molecules. As in form I the hydrogen-bonded chains $\pi\cdots\pi$ -stack on top of each other with a distance of 3.37 Å, resulting in layers along the *b*-axis. Neighbouring layers are generated through the 2_1 -screw operation.

Energy calculations of the polymorphs

Crystals of sufficient size and quality for single-crystal neutron diffraction could not be grown of either of the anhydrous crystal forms, and hence the coordinates of the X-ray structures were utilised for the non-empirical energy calculations using the PACHA algorithm.⁴⁸ Since the hydrogen-atom positions of these structures suffer from the usual X-ray distortion, all hydrogen atoms were added in calculated positions with optimised bond lengths⁵² and their position subsequently optimised sterically and electrostatically. The PACHA algorithm is a fast, *ab initio* method that treats atoms as point charges and is thus a simple approximation to the calculation of lattice energies compared to the high-level algorithms used for polymorph prediction.⁵³⁻⁵⁶ Therefore, the values derived from PACHA cannot be taken as absolute, because small changes in the treatment of the atomic partial charges, as implemented in other algorithms, could have great influence on the resulting calculated lattice energies. However, this simplification allows calculations to be performed within minutes rather than weeks, and thus PACHA presents itself as a rapid and efficient tool for the interpretation of crystal network energies. Due to its limitations, only the trends rather than absolute values are emphasised in the following discussion. For detailed information of the calculations refer to the supporting information.

Both form I and form II have motif 1 in common (see ESI figure S1 and S2), in which the theophylline molecules stack on top of each other interacting through cooperative $\pi\cdots\pi$ stacking and non-cooperative short contacts of the methyl groups. The interaction energies are $+4.1 \text{ kJ mol}^{-1}$ for form I and $+7.8 \text{ kJ mol}^{-1}$ for form II. The difference in energy can be explained by the difference in distance in these stacks (3.86 \AA for form I versus 3.77 \AA for form II), which in the case of form II results in a stronger repulsion of the methyl groups and thus higher energy.

The subsequent stacking of this basic motif 1 is quite different for the two polymorphs. In form I the basic stacks are packed along (0 1 0) with an interaction energy of $-21.5 \text{ kJ mol}^{-1}$ (motif 2). This value is the sum of two different interactions, one being a hydrogen bond between a methyl group and the carbonyl group of the next molecule, while a second hydrogen bond links the ring's acidic $\text{C}_4\text{-H}_{4a}$ to atom N_3 on the next molecule. Finally, the stacks are connected through the conventional hydrogen bond (motif 3) linking $\text{N}_4\text{-H}_4$ with $\text{O}_2=\text{C}_2$ with an energy of $-23.9 \text{ kJ mol}^{-1}$, which can be classified as a medium strength hydrogen bond.⁵⁷

The stacking of motif 1 in form II shows a second stacking motif along (0 0 1) with an interaction energy of $-10.8 \text{ kJ mol}^{-1}$ (motif 2). This interaction is cooperative due to hydrogen bonds between a methyl and a carbonyl group resulting in single hydrogen-bonded chains along the *c*-axis. In packing motif 3, these chains stack according to the σ glide plane resulting in double chains. The interaction energy of -9.6 kJ mol^{-1} means that these chains are slightly less cooperative due to repulsive short interactions between methyl groups. These interactions are located in the (2 0 0) face of the platy crystals (see Figure S3 in ESI), which were found to show dislocation upon cutting and preparation for diffraction experiments. An explanation for this behaviour would be that the crystals show low resistance against shear forces and the layers can slide over each other easily. Motif 4 shows the hydrogen-bonded stacks of motif 1, which are cooperative with $-13.7 \text{ kJ mol}^{-1}$. Even though the values of the hydrogen bonding energies are not comparable, the relative energy of the hydrogen bond to the overall lattice energy is considerably lower in form II than in form I and thus the

hydrogen bond can be assumed to be weaker. This is explicable by the lower electronegativity of the acceptor nitrogen atom compared to that of oxygen. In addition, the hydrogen-bond in form I is shorter in comparison to that in form II (donor-acceptor distance 2.73 Å and 2.79 Å, respectively) even though the bond in form II is more linear than that in form I (bond angle of 174.6° vs. 154.6° based on the optimised hydrogen atom coordinates).

The crystal structures and respective energies give an insight into the lack of interconversion between the two crystal forms of THEO despite their enantiotropic relationship. To transform form II into form I upon heating, not only the existing hydrogen-bond has to be broken but also the molecules have to rearrange significantly to reconnect into new hydrogen-bonded chains. This process resembles partial melting and has indeed been reported to take place only at higher temperatures and over the relatively long time of several hours.²⁸ It is possible that this transition takes place via the gas phase, as THEO sublimates readily at higher temperatures, and although the sublimation product is normally form II, it is likely that above the transition temperature form I nucleates upon resublimation. The transition of form I to form II upon cooling is hindered again by the necessity of rearrangement on the molecular scale. In addition, the hydrogen bond to be broken is considerably stronger, so that the transition requires a very high activation energy unlikely to be provided at lower temperatures at which form II is the stable polymorph.

Taking all calculations into account, the interactions of the 3D network in form I are stronger than those of form II. It is probable that form II is a faster growing crystal form than form I, as the interactions in this crystal form have lower energy and have a higher orientational freedom, as most interactions are single hydrogen bonds compared to the dimerisation in form I (motif 2).

The monohydrate

Even though the monohydrate of theophylline has been extensively studied, no neutron crystal structure has been reported. Crystals of suitable size were grown by evaporation of an aqueous solution and Laue neutron diffraction data were measured on VIVALDI at the Institut Laue-Langevin (Grenoble, France).⁵⁸ In order to obtain the most accurate structural model, the same crystals were initially submitted to X-ray diffraction and the structure redetermined at 120 K. Neutron Laue diffraction data were then collected at 120 K and at 20 K. Details of the two neutron structure refinements are listed in Table 1.

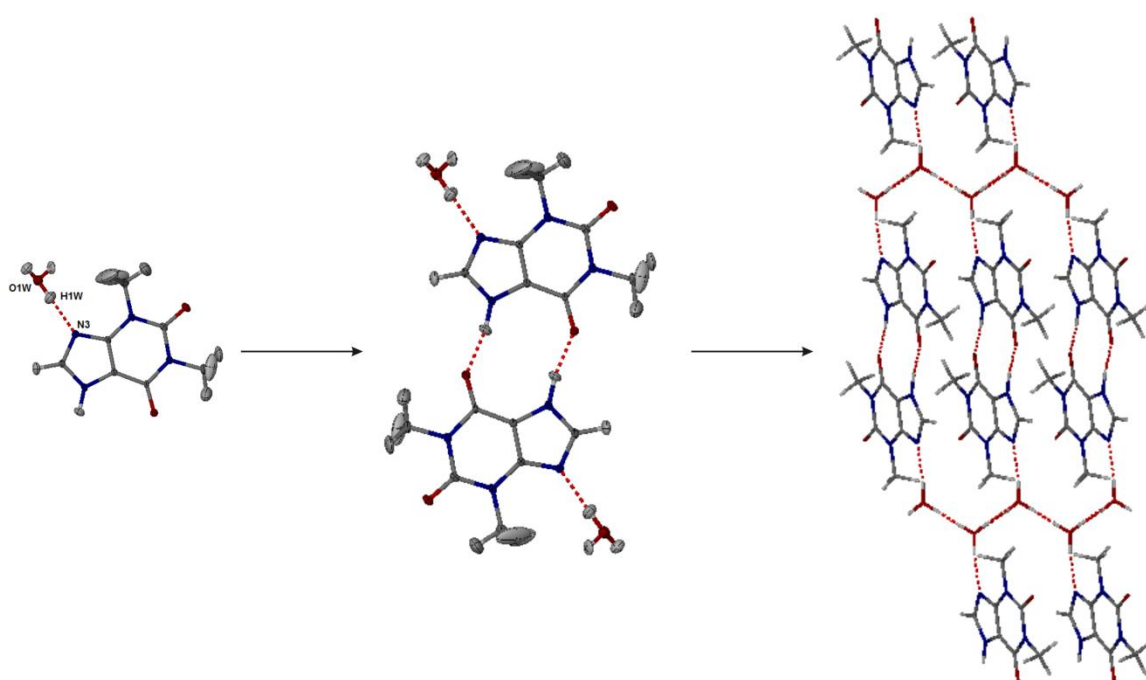


Figure 3 Hydrogen bonding and packing diagram of the THEO monohydrate neutron structure at 120 K. Ellipsoids are drawn at 50% probability. The water hydrogen atoms are disordered.

As described by Sun *et al.*³⁴ the theophylline monohydrate structure consists of theophylline dimers connected through an inversion centre. This results in the formation of two hydrogen bonds from N4-H4 to O1 with an H \cdots O distance of 1.732(9) Å at 120 K and 1.762(19) Å at 20 K. In both cases these interactions are very directional with N-H \cdots O angles of 167.9(8)° and 163.5(15)°, respectively. The distances correlate well with those described by Sutor,³³ who found the N \cdots O distance to be

2.76 Å (*cf.* 2.749(5) Å at 120 K and 2.757(10) Å at 20 K in the present work). This dimerisation is unique in the crystal structures of THEO and can be assumed to play a major role in the formation of the hydrate since it exposes the strongly basic nitrogen atom N3. The dimers are located in layers along the crystallographic a -axis, which show an interplanar distance of 3.26 Å and thus can be assumed to interact through $\pi\cdots\pi$ -stacking. No hydrogen bond exists between these layers. Along the b -axis, the THEO layers are separated through channels of water molecules, which interact with the THEO molecules through one hydrogen bond to N3 (Figure 3). These show a considerably longer H \cdots O distance (1.932(10) Å at 120 K and 1.90(2) Å at 20 K) than the dimer interactions, while being equally linear (171.5(10)° and 172.7(18)°, respectively). It can be assumed that these bonds are weaker than the hydrogen bonds linking the dimeric units together. The second hydrogen atom of the water molecule is disordered over two positions with close to 50% occupancy on each position. Due to the orientation of the water molecules in the channel, they can hydrogen bond either along (1 0 0) or along (-1 0 0) with equal probability. Both possibilities of these hydrogen bonds have an H \cdots O distance around 1.83 Å, with the exception of one hydrogen bond in the 120 K structure being considerably longer with 1.896(17) Å. All of these bonds are very directional with the bond angle well above 170°.

An interesting feature of the monohydrate crystal structures is the disorder in both methyl groups. Sun *et al.* model one of the methyl groups as being statically disordered over two positions by rotation around the methyl carbon atom. The neutron structure at 120 K shows very large atomic displacement parameters (ADP) for the hydrogen atoms of both methyl groups (Figure 4), while both carbon atoms show normal ADPs. Modelling disorder of the hydrogen atoms over two or more sites as would result by static disorder of the methyl group by rotation about the C-C bond resulted in an unstable refinement. Upon cooling to 20 K, the ADPs of the methyl hydrogen atoms are still very large compared to the remaining atoms, but comparison to those of the 120 K structure reveal an overall reduction in size. This points towards dynamic disorder, which can be minimised by cooling of the crystal structure, and will finally contribute to the zero-point motion of the crystal form.

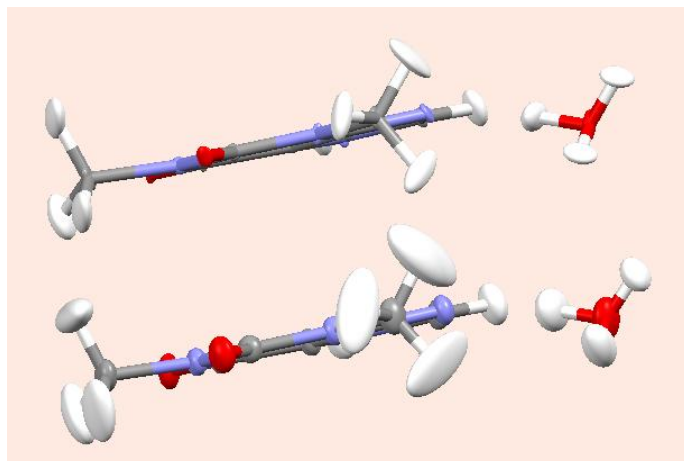


Figure 4 Comparison of the monohydrate structure at 120 K (lower) and at 20 K (upper) with the atomic displacement parameters of the two methyl substituents.

Energy calculations of the monohydrate

The basic motif in the monohydrate is the dimer of THEO molecules (see ESI figure S4), which furthermore are only interacting with another THEO molecule through C-H...O hydrogen bond and with the water molecules. The hydrogen bond in these dimers could be calculated to have an energy of $-15.2 \text{ kJ mol}^{-1}$, thus the total interaction energy of the dimers is $-30.4 \text{ kJ mol}^{-1}$. This interaction energy represents a large amount of the overall lattice energy and is higher than the relative contributions of the hydrogen bonds found in the anhydrous forms I and II. It is thus surprising that the dimer is not the most common motif. Only surprisingly low energetic interactions can be found between these dimers, with the strongest being the C-H...O interaction, which is calculated to have an energy of -2.9 kJ mol^{-1} , due to the long distance of 2.09 \AA (hydrogen to acceptor).

Due to the disorder in the water molecules only an average interaction energy for the homomeric hydrogen bond can be determined. However, at $-33.5 \text{ kJ mol}^{-1}$, this interaction is relatively strong, although still moderate on Jeffrey's scale.⁵⁷ The heteromeric interaction has an energy of -20.3 (H2W) and $-23.2 \text{ kJ mol}^{-1}$ (H3W), values that are higher than the values found by Suihko *et al.* by

molecular modelling using semi-empirical chemical calculations on an optimised model of the X-ray crystal structure of the monohydrate (12.4 kJ mol^{-1}).⁵⁹ However, they are considerably lower than the homomeric interaction energies of the monohydrate. It can be assumed that upon dehydration of the monohydrate, the whole channel clears at once, as the interaction to the host is broken more easily than the homomeric interaction in the water. The resulting dehydrated form would be structurally very closely related to the hydrate, as the THEO dimers remain undisturbed due to the higher homomeric hydrogen-bonding strength. Such dehydration behaviour is reported for drying the THEO monohydrate at low pressure and room temperature to obtain the metastable anhydrous form III, which was found to have a very similar NIR spectrum and powder X-ray diffractogram to the hydrate.⁶⁰ Amado *et al.* even postulate that form III is the direct dehydration product of the monohydrate at any temperature and ambient pressure,⁶¹ which would corroborate our hypothesis of its dimeric structure. The dehydrated form III is reported to undergo rapid transition to form II. This would be understandable because of the destabilising voids left in the crystal structure due to the removal of the water molecules. In addition, the THEO molecules in form III would only be stabilised through very weak interactions other than the dimers, while form II shows a more stabilising crystal network.

The neutron structure of the monohydrate at 20 K reveals that most of the interactions become stronger according to the PACHA calculations. Especially interesting is the decrease of the THEO dimer hydrogen-bonding energy by 12 kJ mol^{-1} to $-27.1 \text{ kJ mol}^{-1}$. In combination with the very strong homomeric water hydrogen bond of $-38.6 \text{ kJ mol}^{-1}$ and the almost unchanged THEO-water interaction of -22.6 and $-22.4 \text{ kJ mol}^{-1}$, the homomeric interactions become more pronounced. These results imply that the dehydration and conservation of the dehydrated crystal structure should be energetically more favoured at lower temperatures, as the interaction between the water and the host molecules weakens. To prove this, dehydration at lower pressures and low temperature would have to be performed, which is to be followed up in future studies.

Conclusion

The single-crystal X-ray structure of theophylline high temperature form I is reported and comparison to the known structure of form II shows that the crystal form is stabilised by different hydrogen bonds and the overall packing changes. Thus these two crystal forms are packing polymorphs.⁵¹ The neutron structure of the monohydrate at 120 K and 20 K verifies the described disorder of one water hydrogen atom position, while the disorder in the methyl groups was found to be of dynamic nature. Lattice energy calculations based on the structural models reveal that the hydrogen bonding energies in the two anhydrous polymorphs vary considerably, as was found for the stabilising packing energies. The hydrogen bonds between the THEO molecules were found to be stronger in form I than in form II. The low conversion rate of form II to form I at higher temperatures can thus be explained by the necessity to break this moderate hydrogen bond and a complete rearrangement of the crystal packing. The reverse transformation has not been observed yet, and can be explained by the necessity to break an even stronger hydrogen bond at lower temperatures, at which it is unlikely to overcome the activation energy of the transition.

The energy calculations on the monohydrate reveal strong homomeric interactions in the water channels and for the theophylline dimers, while the interaction between the two species is comparably weak. From this information the dehydration behaviour can be rationalised and the structure of form III assumed as having the same dimer structure as the monohydrate. The different energies also help to explain the low stability of the hydrate, as only medium interactions have to be overcome to release the incorporated water from the structure. Our neutron single-crystal structure study also cleared the case beyond doubt of disordered hydrogen atom positions in the water molecule to be of static nature, while the hydrogen atoms of the methyl groups are dynamically disordered.

The combination of neutron structures with non-empirical lattice energy calculations proves to be a valuable tool to understand the relationship between crystal structures and results in accurate hydrogen bonding and packing energies. This information is not only improving our understanding of polymorphic and solvated crystal structures but also is essential for designing accurate models for polymorph prediction.

Acknowledgements

We would like to thank EPSRC for funding this study (grant number EP/F063229/1) and the ILL for the allocation of beamtime.

Supporting Information Available

Details of the lattice energy calculations and cif files of the crystal structures are available as electronic supporting information. This information is available free of charge via the Internet at <http://pubs.acs.org/>.

Experimental

Materials

Theophylline was purchased from Sigma-Aldrich and used without any further purification. Form I crystals were crystallised from the melt above 270 °C. Form II crystals were obtained by slow sublimation at 120 °C, while the monohydrate was crystallised by evaporation to dryness of a saturated water solution at room conditions.

Methods

Slurry conversion of THEO form II in methanol

An amount of 500 mg pure form II was slurried in 10 ml of methanol (p.a. standard), stirred at 600 rpm, and characterised daily by Attenuated Total Reflection infrared spectroscopy (Spectrum 100, Perkin Elmer, Cambridge, UK). No conversion was detected after 18 days.

X-ray single-crystal diffraction

Single-crystals of all three crystal forms suitable for structure determination were selected, soaked in perfluoropolyether oil and mounted on Mitegen sample holders. Crystallographic measurements were carried out at 120K using a Bruker SMART CCD 6000 single-crystal diffractometer equipped with an open-flow N₂ Cryostream (Oxford cryosystems) device using a graphite monochromated MoK α radiation ($\lambda = 0.71073\text{\AA}$). For data reduction, the SAINT suite was used, the structures were solved with SHELXS⁶² and refined with SHELXL⁶². All non-hydrogen atoms were treated anisotropically, the hydrogen atoms connected to carbon atoms were added in calculated positions and refined isotropically as riding models. The hydrogen atom bound to the nitrogen was located from the Fourier maps and refined isotropically.

Neutron single-crystal diffraction

A single-crystals of the monohydrate of the size of $2 \times 0.5 \times 0.4 \text{ mm}^3$ was mounted on a V pin with vacuum grease and placed in a helium-flow cryostat on the Very-Intense Vertical-Axis Laue Diffractometer (VIVALDI)⁵⁸ at the Institut Laue-Langevin, Grenoble, France. Data were collected from the stationary crystal at 120 K and 20 K using a white neutron beam with wavelengths between 0.8 and 5 Å. The crystal was rotated 20° between patterns, which were recorded in exposures of 90 minutes. The patterns were indexed using the program LAUEGEN^{63,64} and the reflections integrated using the local program INTEGRATE+⁶⁵ and normalised to a common incident wavelength using the program rearrange. Correction for absorption was deemed unnecessary in view of the small sample volume. The obtained dataset was then refined against the model obtained by X-ray diffraction using SHELXL.⁶² Since only relative unit-cell lengths can be determined by Laue technique, the unit cell at 20 K was estimated by assuming a decrease in each cell axis from 120 K of 1%. All atoms were refined anisotropically.

References

- (1) Mitscherlich, E. *Ann. Chim. Phys.* **1822**, *19*, 350.
- (2) Bernstein, J. *Cryst. Growth Des.* **2011**, *11*, 632.
- (3) Hilfiker, R. *Polymorphism: In the Pharmaceutical Industry*; Wiley-VCH Verlag GmbH & Co. KGaA, Weinheim, Germany, 2006.
- (4) Brittain, H. G. *Polymorphism in Pharmaceutical Solids*; Marcel Dekker Inc.: New York, 1999.
- (5) Bernstein, J. *Polymorphism in Molecular Crystals*; Clarendon Press: Oxford, 2002.
- (6) Bauer, J.; Spanton, S.; Henry, R.; Quick, J.; Dziki, W.; Porter, W.; Morris, J. *Pharm. Res.* **2001**, *18*, 859.
- (7) Cabri, W.; Ghetti, P.; Pozzi, G.; Alpegiani, M. *Org. Process Res. Dev.* **2007**, *11*, 64.
- (8) Nangia, A. In *Encyclopedia of Supramolecular Chemistry - update*; Atwood, J. L., Steed, J. W., Eds.; Taylor & Francis: 2007; Vol. 1:1, p 1.
- (9) Griesser, U. J. In *Polymorphism*; Hilfiker, R., Ed.; Wiley-VCH: Weinheim, Germany, 2006, p 211.
- (10) Barbour, L. J.; Orr, G. W.; Atwood, J. L. *Nature* **1998**, *393*, 671.
- (11) Sansam, B. C. R.; Anderson, K. M.; Steed, J. W. *Cryst. Growth Des.* **2007**, *7*, 2649.
- (12) Doedens, R. J.; Yohannes, E.; Khan, M. I. *Chem. Commun. (Cambridge, U. K.)* **2002**, 62.
- (13) Fucke, K.; Steed, J. W. *Water* **2010**, *2*, 333.
- (14) Fucke, K.; Anderson, K. M.; Filby, M. H.; Henry, M.; Wright, J.; Mason, S. A.; Gutmann, M. J.; Barbour, L. J.; Oliver, C.; Coleman, A. W.; Atwood, J. L.; Howard, J. A. K.; Steed, J. W. *Chemistry - A European Journal* **2011**, *17*, 10259.
- (15) Nicholson, C. E.; Chen, C.; Mendis, B.; Cooper, S. J. *Cryst. Growth Des.* **2011**, *11*, 363.
- (16) Bernstein, J. *Polymorphism in Molecular Crystals*; Oxford University Press, Oxford, UK, 2002.
- (17) Price, S. L. *Acc. Chem. Res.* **2009**, *42*, 117.
- (18) Braun, D. E.; Karamertzanis, P. G.; Arlin, J. B.; Florence, A. J.; Kahlenberg, V.; Tocher, D. A.; Griesser, U. J.; Price, S. L. *Cryst. Growth Des.* **2011**, *11*, 210.
- (19) Braun, D. E.; Karamertzanis, P. G.; Price, S. L. *Chem. Commun. (Cambridge, U. K.)* **2011**, *47*, 5443.
- (20) Foster, J. A.; Piepenbrock, M. O. M.; Lloyd, G. O.; Clarke, N.; Howard, J. A. K.; Steed, J. W. *Nature Chem.* **2010**, *2*, 1037.
- (21) Kossel, A. *Berichte der Deutschen Chemischen Gesellschaft* **1888**, *21*, 2164
- (22) *Pharmacopoeia Europaea 6.8*; Deutscher Apotheker Verlag, Stuttgart & Govi-Verlag GmbH, Eschborn; Vol. 5.08.
- (23) *United States Pharmacopoeia Vol 32*.
- (24) Duddu, S. P.; Das, N. G.; Kelly, T. P.; Sokoloski, T. D. *Int. J. Pharm.* **1995**, *114*, 247.
- (25) De Smidt, J. H.; Fokkens, J. G.; Grijseels, H.; Crommelin, D. J. A. J. *J. Pharm. Sci.* **1986**, *75*, 497.
- (26) Otsuka, M.; Kaneniwa, N.; Kawakami, K.; Umezawa, O. *J. Pharm. Pharmacol.* **1991**, *43*, 226.
- (27) Otsuka, M.; Kaneniwa, N.; Otsuka, K.; Kawakami, K.; Umezawa, O. *Drug Dev. Ind. Pharm.* **1993**, *19*, 541.
- (28) Griesser, U. J.; Szlagiewicz, M.; Hofmeier, U. C.; Pitt, C.; Cianferani, S. J. *Therm. Anal. Calorim.* **1999**, *57*, 45.
- (29) Burger, A.; Ramberger, R. *Mikrochim. Acta* **1979**, *2*, 273.

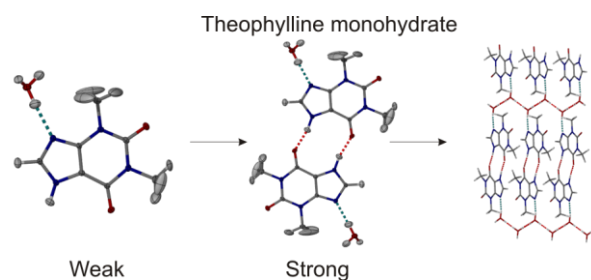
- (30) Suzuki, E.; Shimomura, K.; Sekiguchi, K. *Chem. Pharm. Bull.* **1989**, *37*, 493.
- (31) Naqvi, A. A.; Bhattacharyya, G. C. *J. Appl. Crystallogr.* **1981**, *14*, 464.
- (32) Ebisuzaki, Y.; Boyle, P. D.; Smith, J. A. *Acta Crystallographica Section C-Crystal Structure Communications* **1997**, *53*, 777.
- (33) Sutor, D. J. *Acta Crystallogr.* **1958**, *11*, 83.
- (34) Sun, C.; Zhou, D.; Grant, D. J. W.; Young Junior, V. G. *Acta Crystallogr., Sect. E: Struct. Rep. Online* **2002**, *58*, o368
- (35) Phadnis, N. V.; Suryanarayanan, R. *J. Pharm. Sci.* **1997**, *86*, 1256.
- (36) Matsuo, K.; Matsuoka, M. *Cryst. Growth Des.* **2007**, *7*, 411.
- (37) Das, B.; Baruah, J. B. *Cryst. Growth Des.* **2011**, *11*, 278.
- (38) Schultheiss, N.; Roe, M.; Boerrigter, S. X. M. *CrystEngComm* **2011**, *13*, 611.
- (39) Lu, J.; Rohani, S. *J. Pharm. Sci.* **2010**, *99*, 4042.
- (40) Chattoraj, S.; Shi, L. M.; Sun, C. C. *CrystEngComm* **2010**, *12*, 2466.
- (41) Childs, S. L.; Stahly, G. P.; Park, A. *Mol. Pharmaceutics* **2007**, *4*, 323.
- (42) Karki, S.; Friscic, T.; Jones, W.; Motherwell, W. D. S. *Mol. Pharmaceutics* **2007**, *4*, 347.
- (43) Seton, L.; Khamar, D.; Bradshaw, I. J.; Hutcheon, G. A. *Cryst. Growth Des.* **2010**, *10*, 3879.
- (44) Khamar, D.; Seton, L.; Bradshaw, I.; Hutcheon, G. *J. Pharm. Pharmacol.* **2010**, *62*, 1333.
- (45) Roy, C.; Vega-Gonzalez, A.; Subra-Paternault, P. *Int. J. Pharm.* **2007**, *343*, 79.
- (46) Roy, C.; Vrel, D.; Vega-Gonzalez, A.; Jestin, P.; Laugier, S.; Subra-Paternault, P. *J. Supercrit. Fluids* **2011**, *57*, 267.
- (47) Eddleston, M. D.; Bithell, E. G.; Jones, W. *J. Pharm. Sci.* **2010**, *99*, 4072.
- (48) Henry, M. *ChemPhysChem* **2002**, *3*, 561.
- (49) During the reviewing process of this manuscript the crystal structure of form I has been published (DOI: 10.1021/cg2008478).
- (50) Anderson, K. M.; Day, G. M.; Paterson, M. J.; Byrne, P.; Clarke, N.; Steed, J. W. *Angew. Chem., Int. Ed.* **2008**, *47*, 1058.
- (51) Grant, D. J. W. In *Polymorphism in Pharmaceutical Solids*; Brittain, H. G., Ed.; Marcel Dekker Inc.: New York, 1999; Vol. 95, p 1.
- (52) Gailar, N.; Plyler, E. K. *J. Chem. Phys.* **1956**, *24*, 1139.
- (53) Day, G. M.; Motherwell, W. D. S.; Jones, W. *Phys. Chem. Chem. Phys.* **2007**, *9*, 1693.
- (54) Day, G. M.; Motherwell, W. D. S.; Ammon, H. L.; Boerrigter, S. X. M.; Della Valle, R. G.; Venuti, E.; Dzyabchenko, A.; Dunitz, J. D.; Schweizer, B.; van Eijck, B. P.; Erk, P.; Facelli, J. C.; Bazterra, V. E.; Ferraro, M. B.; Hofmann, D. W. M.; Leusen, F. J. J.; Liang, C.; Pantelides, C. C.; Karamertzanis, P. G.; Price, S. L.; Lewis, T. C.; Nowell, H.; Torrisi, A.; Scheraga, H. A.; Arnautova, Y. A.; Schmidt, M. U.; Verwer, P. *Acta Crystallogr., Sect. B: Struct. Sci.* **2005**, *61*, 511.
- (55) Kendrick, J.; Leusen, F. J. J.; Neumann, M. A.; van de Streek, J. *Chemistry* **2011**, *17*, 10736.
- (56) Bardwell, D. A.; Adjiman, C. S.; Arnautova, Y. A.; Bartashevich, E.; Boerrigter, S. X. M.; Braun, D. E.; Cruz-Cabeza, A. J.; Day, G. M.; Della Valle, R. G.; Desiraju, G. R.; van Eijck, B. P.; Facelli, J. C.; Ferraro, M. B.; Grillo, D.; Habgood, M.; Hofmann, D. W. M.; Hofmann, F.; Jose, K. V. J.; Karamertzanis, P. G.; Kazantsev, A. V.; Kendrick, J.; Kuleshova, L. N.; Leusen, F. J. J.; Maleev, A. V.; Misquitta, A. J.; Mohamed, S.; Needs, R. J.; Neumann, M. A.; Nikylov, D.; Orendt, A. M.; Pal, R.; Pantelides, C. C.; Pickard, C. J.; Price, L. S.; Price, S. L.; Scheraga, H. A.; van de Streek, J.; Thakur, T. S.; Tiwari, S.; Venuti, E.; Zhitkov, I. K. *Acta Crystallogr., Sect. B: Struct. Sci.* **2011**, *67*, 535.
- (57) Jeffrey, G. A. *An Introduction to Hydrogen Bonding*; 1st ed.; OUP: Oxford, 1997.
- (58) McIntyre, G. J.; Lemee-Cailleau, M. H.; Wilkinson, C. *Physica B* **2006**, *385-86*, 1055.
- (59) Suihko, E.; Ketolainen, J.; Poso, A.; Ahlgren, M.; Gynther, J.; Paronen, P. *Int. J. Pharm.* **1997**, *158*, 47.
- (60) Vora, K. L.; Buckton, G.; Clapham, D. *Eur. J. Pharm. Sci.* **2004**, *22*, 97.

- (61) Amado, A. M.; Nolasco, M. M.; Ribeiro-Claro, P. J. A. *J. Pharm. Sci.* **2007**, *96*, 1366.
- (62) Sheldrick, G. M. *Acta Crystallogr., Sect. A: Found. Crystallogr.* **2008**, *A64*, 112.
- (63) Campbell, J. W. *J. Appl. Crystallogr.* **1995**, *28*, 228.
- (64) Campbell, J. W.; Hao, Q.; Harding, M. M.; Nguti, N. D.; Wilkinson, C. *J. Appl. Crystallogr.* **1998**, *31*, 496.
- (65) Wilkinson, C.; Khamis, H. W.; Stansfield, R. F. D.; McIntyre, G. J. *J. Appl. Crystallogr.* **1988**, *21*, 471.

For Table of Contents Use Only

New insights into an Old Molecule: Interaction Energies of Theophylline Crystal Forms

Katharina Fucke, Garry J. McIntyre, Clive Wilkinson, Marc Henry, Judith A.K. Howard, Jonathan W. Steed



The asthma therapeutic theophylline exists in three anhydrous polymorphs and a monohydrate. The energetic relationship between forms I and II is investigated using the partial charges and chemical hardness analysis (PACHA) algorithm. PACHA investigations based on the neutron single crystal structure of the monohydrate reveal that the homomeric interactions are stronger than those of the water with the host molecules.